# Structural Phase Transition and Magnetic-Field Effect on the Modulated Structure in GdBaCo$_2$O$_{5+\delta}$ ($\delta < 0.5$)

T. Asaka,[1] N. Abe,[2] T. Kudo,[1] K. Fukuda,[1] K. Kimoto,[3] Y. Matsui,[3] N. Ishizawa,[4] and T. Arima[2]

[1]*Department of Materials Science and Engineering, Nagoya Institute of Technology, Nagoya 466-8555, Japan*
[2]*Department of Advanced Materials Science, University of Tokyo, Kashiwa 277-8561, Japan*
[3]*National Institute for Materials Science, Tsukuba 305-0044, Japan*
[4]*Advanced Ceramics Research Center, Nagoya Institute of Technology, Tajimi 507-0071, Japan*

We investigated the crystal structures of an ordered perovskite-type cobaltate, GdBaCo$_2$O$_{5+\delta}$ ($\delta < 0.5$), at elevated temperatures by transmission electron microscopy. Above the magnetic ordering temperature, we observed a first-order structural phase transition between the low-temperature tetragonal $3a_p \times 3a_p$ and high-temperature orthorhombic $1a_p \times 2a_p$ superstructure phases (where $a_p$ is the perovskite-unit cell). Upon the application of a magnetic field, an incommensurate phase emerges around the structural phase-transition temperature, which indicates a magnetic-field-induced structural phase transition via no magnetic ordering in the ordered perovskite-type cobaltate.

A crystal structure is intimately related to its macroscopic physical properties, particularly in materials with correlated electrons. Nontrivial structural phase transitions associated with electronic and magnetic states are often found in correlated-electron systems. Occasionally, superstructure or modulated-structure phases may emerge, engaged with ordering or density waves of charge, orbital, or spin degree of freedom [1–3]. Furthermore, by applying external fields, the modulated structures are likely to be additionally modified and modulated through changes in the ordering or density waves. Such a phenomenon has been found in many correlated-electron systems: magnetoelectric oxides such as TbMnO$_3$ [4] and Ba$_{0.5}$Sr$_{1.5}$Zn$_2$Fe$_{12}$O$_{22}$ [5], spiral antiferromagnets such as Ba$_2$CuGe$_2$O$_7$ [6], one-dimensional antiferromagnets such as Cu(C$_6$D$_5$COO)$_2 \cdot$3D$_2$O [7], compounds with charge density such as TaS$_3$ [8], and spin-Peierls compounds such as CuGeO$_3$ [9] and tetrathiafulvalence-Cu-*bis*-dithiolene (TTF-CuBDT) [10]. Note that such field effects were observed exclusively in ordered states. The superstructure or modulated-structure phases involved with electronic and magnetic states can provide an appropriate stage for cross correlation effects.

The $A$-site ordered perovskite-type cobaltates with the general formula $R$BaCo$_2$O$_{5+\delta}$ ($R$ = lanthanoid elements or Y, $0 \le \delta \le 1$) have attracted considerable attention because of their unusual electric and magnetic properties such as magnetoresistance [11–15] and insulator-to-metal transitions (I-M transitions) [11,12,16]. The fundamental crystal structure of $R$BaCo$_2$O$_{5+\delta}$ is regarded as a layered structure which is composed of a stacking of [$RO_\delta$] − [CoO$_2$] − [BaO] − [CoO$_2$] along the $c$ axis [12,17,18]. Consequently, the perovskite-unit cell, $a_p$, is doubled along the $c$ axis. The $RO_\delta$ layers accommodate the oxygen deficiency. Therefore, each oxygen site in the $RO_\delta$ layers

is occupied by either an O ion or a vacancy. This gives rise to the formation of CoO$_6$ octahedra and CoO$_5$ pyramids. Depending on $\delta$, O ions and vacancies (i.e., octahedra and pyramids) are ordered concomitantly with changes in the symmetry: $3a_p \times 3a_p \times 2a_p$ (332) for $\delta = 0.25$–0.44 [12,16–20], $1a_p \times 2a_p \times 2a_p$ (122) for $\delta = 0.45$–0.55 [11,12,14,20–23], and $2a_p \times 2a_p \times 2a_p$ (222) for $\delta \sim 0.75$ [24], which corresponds to tetragonal ($P4/mmm$), orthorhombic ($Pmmm$), and tetragonal ($P4/mmm$) symmetries, respectively.

The parameter $\delta$ also determines the electric and magnetic properties. For example, the 122 phase with $0.45 \le \delta \le 0.55$ exhibits I-M transition at $T_{IM} = 290$–360 K (for $R$ = Pr to Ho and Y) [11,12,14–16,22,25–27]. Interestingly, it is not accompanied by magnetic ordering, whereas various magnetically ordered states appear at low temperatures, such as a noncollinear antiferromagnetic order and a spin state order with aligned magnetic moments [13,19,20,23,28–36]. However, there are no reports on the I-M transition for the 332 phase. In this Letter, we report a thermally induced structural phase transition (SPT) in GdBaCo$_2$O$_{5+\delta}$ ($\delta < 0.5$) between the tetragonal $3a_p \times 3a_p$ and orthorhombic $1a_p \times 2a_p$ superstructure phases. Although these phases do not exhibit any magnetic ordering, SPT exhibits a significant susceptibility to magnetic fields, suggesting a correlation between SPT and electronic states.

Single crystals of GdBaCo$_2$O$_{5+\delta}$ were grown by a floating-zone method, following Ref. [26]. Single-crystal x-ray diffraction data acquired separately indicate that $\delta$ in the present crystal is ~0.38 [37]. With decreasing temperature, the crystal undergoes two-step magnetic phase transitions from a paramagnetic phase to magnetically ordered phases at ~290 K and ~230 K [37]. For transmission electron microscopy (TEM), the crystals were

crushed in an agate mortar and the fragments were dispersed in ethanol and cast onto a TEM specimen grid. The specimens were examined using a conventional electron microscope and a Lorentz electron microscope for magnetic-field and field-free measurements, respectively. Both microscopes were operated at 300 kV. A magnetic field between 0 and 2 T was applied using pole pieces of the electromagnetic objective lens of the conventional electron microscope [5,38]. Note that the magnitude of the magnetic field in a low-field range (including ∼0 T) might be underestimated because of the residual field of the pole pieces of the objective lens of the conventional electron microscope.

In Fig. 1(a), we show a [001]-zone electron diffraction pattern of a sample in zero field at room temperature. Sharp superstructure reflections with modulation wave vectors of $q_1 = (\alpha, 0, 0)$ and $q_2 = (0, \alpha, 0)$ ($\alpha = 0.336(2)$) are observed. The value of $\alpha$ is fairly close to a commensurate value $1/3$. The pattern of the superstructure reflections with the $q_1$ and $q_2$ wave vectors appears two dimensional with tetragonal symmetry. These results indicate that the crystal has essentially a $3a_p \times 3a_p$ superstructure. In fact, we successfully analyzed the crystallographic structure with the $3 \times 3$ superstructure, where O ions and vacancies are ordered in a threefold period along both the tetragonal $a_1$ and $a_2$ axes in the $GdO_\delta$ layer, as shown in Fig. 1(b) [37]. This result agrees with previous reports on the 332 phase [12,16–20]. The $3 \times 3$ superstructure is nearly commensurate with the fundamental lattice. To clarify the evolution of the superstructure with temperature, we
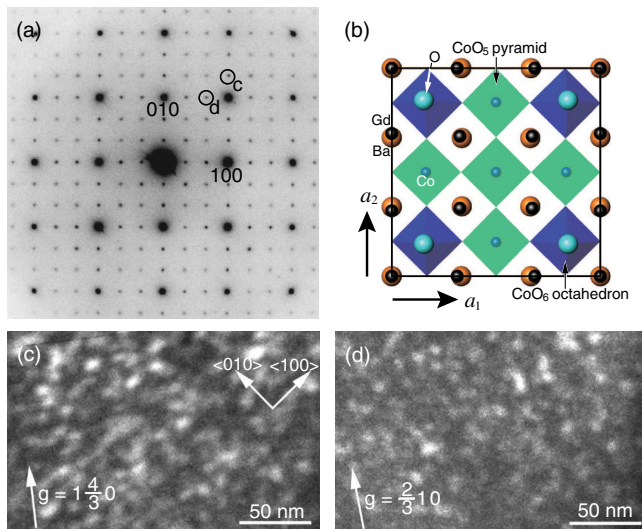


FIG. 1 (color online).  Crystal structure of $GdBaCo_2O_{5+\delta}$ ($\delta \sim 0.38$). (a) [001]-zone electron diffraction pattern obtained in zero field at room temperature. The superstructure reflections with modulation wave vectors of ($\sim 1/3, 0, 0$) and (0, $\sim 1/3, 0$) are evident. (b) Schematic of $GdBaCo_2O_{5+\delta}$ with the $3 \times 3$ superstructure, representing oxygen or vacancy ordering. Dark-field images formed with the superstructure spots of (c) $1\frac{\tilde{-4}}{3}0$ and (d) $\frac{\tilde{-2}}{3}10$, respectively.

performed dark-field imaging using two superstructure spots. Figures 1(c) and 1(d) show [001]-zone dark-field images of the same area in the crystal at room temperature, formed with the superstructure spots of $1\frac{\tilde{-4}}{3}0$ (one of the modulations in the tetragonal $a_2^*$ direction) and $\frac{\tilde{-2}}{3}10$ (one of the modulations in the $a_1^*$ direction), respectively. Bright parts are domains with the structural modulations of (c) $q_2$ or (d) $q_1$. Dark lines and regions indicate antiphase boundaries and disordered regions with respect to the threefold superstructure order along the respective crystal axes. Bright domains in each image are several tens of nanometers in size. The domain distributions in these two images do not coincide with each other and are not complementary. This suggests that the $q_1$ and $q_2$ modulations do not have an identical spatial correlation and a perfect $3 \times 3$ superstructure, but form a *pseudo* two-dimensional modulation.

Figure 2 shows the temperature profiles of electron diffraction patterns. Upon heating from 300 K, weak superstructure reflections with modulation wave vectors of $(1/2, 0, 0)$ and $(0, 1/2, 0)$ emerge around 450 K [Fig. 2(b)]. As the temperature increases, the intensity of the twofold superstructure reflections increases, whereas that of the $q_1$ and $q_2$ superstructure reflections decreases [Fig. 2(c)]. Eventually, the $q_1$ and $q_2$ superstructure reflections vanish [Fig. 2(d)]. Note that the measured temperatures were probably higher by 30–80 K than the true sample temperature, because the measured sample fragments were mounted on a carbon-coated polymer film of a TEM specimen grid.

In the electron diffraction pattern obtained at 480 K [Fig. 2(e)], we observe a split of the fundamental diffraction spots in the higher-order region, whereas the twofold superstructure spots do not split. This observation indicates a twin structure in the high-temperature phase, in which the crystal structure is distorted orthorhombically and exhibits a $1 \times 2$ superstructure. This superstructure is characterized by the reciprocal superstructure-unit cell as indicated by the dashed frames in Fig. 2(e). We acquired dark-field images for the $1 \times 2$ superstructure state. Figures 2(f) and 2(g) show dark-field images formed with the $0\frac{1}{2}0_A$ and $0\frac{1}{2}0_B$ superstructure spots, respectively. The antiphase domains in the both images are several tens of nanometers in size, which is comparable to that in the $3 \times 3$ superstructure in the low-temperature phase. Furthermore, the domains organize bandlike structures, denoted as bands $A$ and $B$ in Figs. 2(f) and 2(g), respectively. Comparing these images, the respective structures show an alternating and complementary stripelike array. This indicates a twin structure with respect to the fundamental structure, which is defined by the $1 \times 2$ superstructure. We conclude that, as a function of temperature, the compound undergoes SPT between the $3 \times 3$ and $1 \times 2$ superstructure phases through the coexistence state. As mentioned above, such SPT has been observed only as a function of oxygen content $\delta$, so far. Here, from only our electron diffraction study, we cannot determine whether the present $1 \times 2$ superstructure
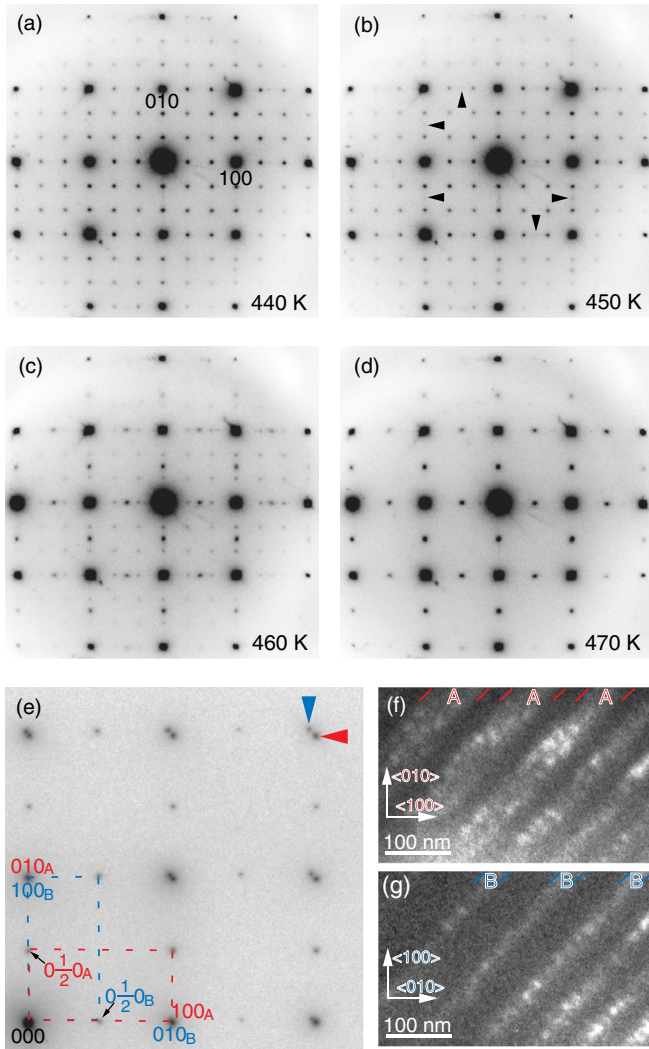
FIG. 2 (color online).   Temperature profile of [001]-zone electron diffraction patterns obtained at zero field at (a) 440 K, (b) 450 K, (c) 460 K, and (d) 470 K. Arrowheads in panel (b) indicate superstructure spots with wave vectors of $(1/2, 0, 0)$ and $(0, 1/2, 0)$. (e) [001]-zone electron diffraction obtained at 480 K. Arrowheads indicate a split of the fundamental diffraction spots in the higher-order region, indicating the presence of orthorhombically distorted twin variants. Dashed frames represent reciprocal unit cells of the $1 \times 2$ superstructure. [110]-zone dark-field images formed with (f) $0\frac{1}{2}0_A$ and (g) $0\frac{1}{2}0_B$ superstructure spots in (e). These images were obtained from the same part of the sample.

phase is identical to the 122 phase, as previously reported for the compounds with $\delta \sim 0.5$ [11,12]. A single-crystal x-ray diffraction analysis at 507 K reveals that the $1 \times 2$ phase has an orthorhombic structure ($Pmmm$) with $a = 3.8687(5)$ Å, $b = 7.8718(8)$ Å, and $c = 7.5883(15)$ Å, being isostructural with those reported for the 122 phase [22,39]. The phase transition between the phases with two discontinuous modulation wave vectors can only be of a first order. The observed coexistence of the low-temperature $3 \times 3$ and high-temperature $1 \times 2$ phases around SPT is a natural consequence of the first-order transition.
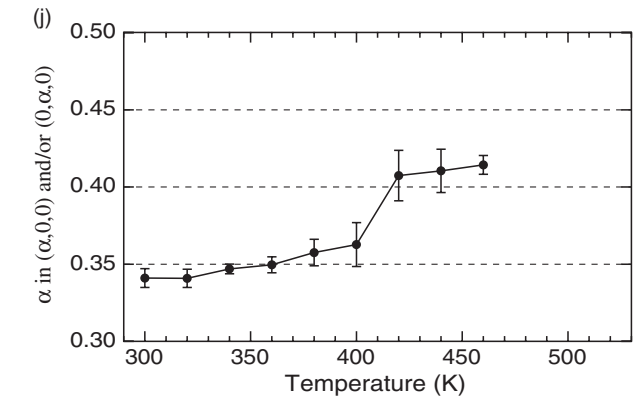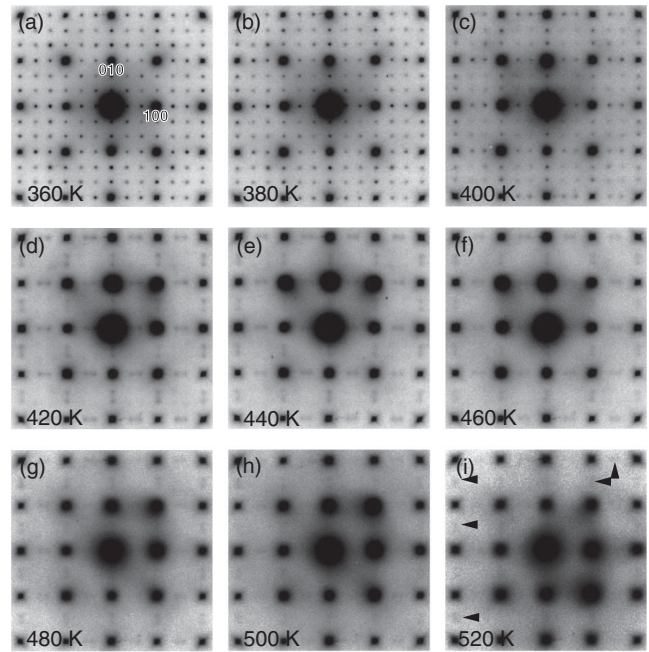


FIG. 3.   Temperature profile of [001]-zone electron diffraction patterns in a magnetic field of $\sim 2$ T, obtained at (a) 360 K, (b) 380 K, (c) 400 K, (d) 420 K, (e) 440 K, (f) 460 K, (g) 480 K, (h) 500 K, and (i) 520 K. Arrowheads indicate diffuse scattering with modulation wave vectors of $(\sim 1/2, 0, 0)$ and $(0, \sim 1/2, 0)$. (j) Temperature dependence of $\alpha$ on the modulation wave vector $q = (\alpha, 0, 0)$ and/or $(0, \alpha, 0)$ in a magnetic field of $\sim 2$ T.

When a sample is heated in a magnetic field, the present SPT exhibits significantly different behavior in the $q$ vectors from that in zero field. In a magnetic field of $\sim 2$ T, the $\alpha$ value for $q_1$ and $q_2$ vectors tends to increase toward 0.5 as the temperature increases (field warming), whereas the intensities of $q_1$ and $q_2$ superstructure reflections decrease, as shown in Figs. 3(a)–3(d). Upon further warming, these become diffuse scattering and approach to $q_1 = (1/2, 0, 0)$ and $q_2 = (0, 1/2, 0)$ [Figs. 3(e)–3(i)]. This result signifies the evolution of short-range order with $q = (\sim 1/2, 0, 0)$ and/or $(0, \sim 1/2, 0)$. We show the temperature dependence of $\alpha$ for the $q$ vectors at $\sim 2$ T in Fig. 3(j). The modulation wave vectors exhibit a considerable incommensurability, which is not observed for the zero-field warming. Note that the fundamental structure maintains a tetragonal lattice

system, showing no difference between the lattice parameters of $a_{p1}$ and $a_{p2}$ in the simple perovskite unit-cell notation, during the structural phase transition in magnetic fields. Moreover, we observed no twin structure due to the orthorhombic distortion in contrast to the high-temperature phase in zero field. The crystal structure belongs to the five-dimensional superspace group $P4/mmm(\alpha 00)0000$ $(0\alpha 0)0000$, $\alpha = 0.336(2)$–0.5, which is identical with that of the 332 phase analyzed as an incommensurate structure in Ref. [37]. We attribute the phase with large incommensurability to the emergence of nanodomains with the $1 \times 2$ (or $2 \times 1$) superstructure, which would be embryos of the high-temperature $1 \times 2$ phase.

We also find that, at a fixed temperature, the modulation wave vectors change under an applied magnetic field. Figure 4 shows the magnetic-field dependence of $\alpha$ at 380 K and 410 K. The $q$ vector shows a linear change between $\alpha \sim 0.35$ and $\sim 0.38$ with increasing magnetic field at 410 K, whereas at 380 K, it is relatively constant. The value $\alpha \sim 0.38$ at 1.6 T is certainly close to that expected around 410 K in Fig. 3 for field warming at $\sim 2$ T. In addition, for increasing magnetic field, the superstructure reflections weaken and change to diffuse scattering, as shown in the inset of Fig. 4. Meanwhile, the fundamental structure seems to maintain a tetragonal structure, similar to that in SPT in the abovementioned field-warming experiments. After the field sweep, the modulation $\alpha$ of superstructure reflections returns to $\alpha \sim 0.35$ at zero field [40]. These results suggest that a magnetic field accelerates nucleation of embryos with $q = (\sim 1/2, 0, 0)$ or $(0, \sim 1/2, 0)$ and fragments the long-range ordered domains with $q = (\sim 1/3, 0, 0)$ and $(0, \sim 1/3, 0)$, similar to that in the abovementioned SPT in the field-warming process. We demonstrate that, by the application of a magnetic field, the incommensurability in

this compound becomes tunable and the short-range order can be stabilized.

The large magnetic-field effect indicates that, in spite of the absence of the magnetic order, the present SPT should involve the electron system in this crystal. We assume two possible origins of the present SPT: a spin state transition (SST) and a transformation of a charge modulation (TCM). According to previous reports, SST in the $\delta \sim 0.5$ compounds (122 phase) is characterized by the transformation from low- or intermediate-spin states to a high-spin state of Co ions, particularly at the octahedral sites in a warming process [21–23,32,36,39]. Variations in the Co-O bond lengths and a symmetry change have been observed at SST [25,30,32,34,41,42]. Incidentally, SST has been proposed as a possible origin for the I-M transition observed in the $\delta \sim 0.5$ compounds, so called spin blockade mechanism [27,43]. On the other hand, SST in the 332 phase has not been reported so far. Since the spin state in transition metal oxides is closely related to the microscopic metal-ligand environments, i.e., the crystal (ligand) fields and Hund coupling, a similar SST can be expected to take place also in the 332 phase which contains the same metal-ligand species as the 122 phase: $CoO_5$ pyramids and $CoO_6$ octahedra. In fact, on-going *in situ* single-crystal x-ray diffraction studies on the present crystal have revealed distinct changes in the Co-O bond lengths of $CoO_5$ pyramids and $CoO_6$ octahedra at SPT, which apparently suggests SST. Concerning the TCM origin, single-crystal x-ray diffraction study has demonstrated that the low-temperature $3 \times 3$ phase exhibits a clear charge modulation according to the oxygen or vacancy ordering [37]. The threefold charge modulation is replaced by a stripe-type modulation in the high-temperature $1 \times 2$ phase. In other words, TCM takes place at SPT. We believe that the present SPT is induced by SST or TCM or their combination. The SPT behavior in a magnetic field might be interpreted by phase stability of the high-spin state of Co ions. Magnetic-field-induced low-spin-to-high-spin state transitions in various cobalt compounds have been reported [44–46]. These reports indicate that magnetic fields often stabilize the high-spin state. The emergence and development of the $1 \times 2$ or $2 \times 1$ superstructural nanodomains with the application of a magnetic field might be due to the effective stimulation of locally disarrayed regions with respect to the $3 \times 3$ superstructural order such as at the antiphase boundaries.

To summarize, by varying the temperature, we found a structural phase transition between the $3a_p \times 3a_p$ and $1a_p \times 2a_p$ superstructure phases in $GdBaCo_2O_{5+\delta}$. This structural phase transition is strongly affected by an applied magnetic field. The observed magnetic-field effect on the modulated structure in the paramagnetic state is a novel phenomenon in transition metal oxides, as far as we know, where a correlation among crystal structure, charge, and spin would play a key role. To clarify details of the structural phase transition, we performed *in situ* single-crystal x-ray diffraction as a function of temperature.



FIG. 4 (color online). Magnetic field dependence of $\alpha$ for modulation wave vector $q = (\alpha, 0, 0)$ and/or $(0, \alpha, 0)$ at 380 K (square symbols) and 410 K (circular symbols). The respective regression lines were drawn to guide the eye. The inset is an electron diffraction pattern taken at 410 K and applied magnetic field of 1.6 T. The electron diffraction pattern is slightly distorted due to a particular lens condition [40].

———————

[1] J. M. Tranquada, B. J. Sternlieb, J. D. Axe, Y. Nakamura, and S. Uchida, Nature (London) **375**, 561 (1995).

[2] C. H. Chen, S.-W. Cheong, and A. S. Cooper, Phys. Rev. Lett. **71**, 2461 (1993).

[3] C. H. Chen and S.-W. Cheong, Phys. Rev. Lett. **76**, 4042 (1996).

[4] T. Arima, T. Goto, Y. Yamasaki, S. Miyasaka, K. Ishii, M. Tsubota, T. Inami, Y. Murakami, and Y. Tokura, Phys. Rev. B **72**, 100102(R) (2005).

[5] T. Asaka, X. Z. Yu, Y. Hiraoka, K. Kimoto, T. Hirayama, T. Kimura, and Y. Matsui, Phys. Rev. B **83**, 130401(R) (2011).

[6] A. Zheludev, S. Maslov, G. Shirane, Y. Sasago, N. Koide, and K. Uchinokura, Phys. Rev. Lett. **78**, 4857 (1997).

[7] D. C. Dender, P. R. Hammar, D. H. Reich, C. Broholm, and G. Aeppli, Phys. Rev. Lett. **79**, 1750 (1997).

[8] K. Inagaki, M. Tsubata, K. Higashiyama, K. Ichimura, S. Tanda, K. Yamamoto, N. hanasaki, N. Ikeda, Y. Nogami, T. Ito, and H. Toyokawa, J. Phys. Soc. Jpn. **77**, 093708 (2008).

[9] V. Kiryukhin and B. Keimer, Phys. Rev. B **52**, R704 (1995).

[10] V. Kiryukhin, B. Keimer, and D. E. Moncton, Phys. Rev. Lett. **74**, 1669 (1995).

[11] C. Martin, A. Maignan, D. Pelloquin, N. Nguyen, and B. Raveau, Appl. Phys. Lett. **71**, 1421 (1997).

[12] A. Maignan, C. Martin, D. Pelloquin, N. Nguyen, and B. Raveau, J. Solid State Chem. **142**, 247 (1999).

[13] A. A. Taskin, A. N. Lavrov, and Y. Ando, Phys. Rev. Lett. **90**, 227201 (2003).

[14] A. A. Taskin, A. N. Lavrov, and Y. Ando, Phys. Rev. B **71**, 134414 (2005).

[15] E. S. Vlakhov, N. Kozlova, L. S. Lobanovskii, R. Wawryk, and K. A. Nenkov, Phys. Rev. B **84**, 184440 (2011).

[16] D. Akahoshi and Y. Ueda, J. Solid State Chem. **156**, 355 (2001).

[17] W. Zhou, Chem. Mater. **6**, 441 (1994).

[18] W. Zhou, C. T. Lin, and W. Y. Liang, Adv. Mater. **5**, 735 (1993).

[19] D. D. Khalyavin, A. M. Balagurov, A. I. Beskrovnyi, I. O. Troyanchuk, A. P. Sazonov, E. V. Tsipis, and V. V. Kharton, J. Solid State Chem. **177**, 2068 (2004).

[20] D. D. Khalyavin, D. N. Argyriou, U. Amann, A. A. Yaremchenko, and V. V. Kharton, Phys. Rev. B **75**, 134407 (2007).

[21] Y. Moritomo, T. Akimoto, M. Takeo, A. Machida, E. Nishibori, M. Takata, M. Sakata, K. Ohoyama, and A. Nakamura, Phys. Rev. B **61**, R13325 (2000).

[22] S. Roy, M. Khan, Y. Q. Guo, J. Craig, and N. Ali, Phys. Rev. B **65**, 064437 (2002).

[23] F. Fauth, E. Suard, V. Caignaert, and I. Mirebeau, Phys. Rev. B **66**, 184421 (2002).

[24] C. Frontera, J. L. García-Muñoz, A. E. Carrillo, C. Ritter, D. Martin y Marero, and A. Caneiro, Phys. Rev. B **70**, 184428 (2004).

[25] Yu. P. Chernenkov, V. P. Plakhty, A. G. Gukasov, S. N. Barilo, S. V. Shiryaev, G. L. Bychkov, V. Hinkov, V. I. Fedorov, and V. A. Chekanov, Phys. Lett. A **365**, 166 (2007).

[26] T. Saito, T. Arima, Y. Okimoto, and Y. Tokura, J. Phys. Soc. Jpn. **69**, 3525 (2000).

[27] A. Maignan, V. Caignaert, B. Raveau, D. Khomskii, and G. Sawatzky, Phys. Rev. Lett. **93**, 026401 (2004).

[28] J. C. Burley, J. F. Mitchell, S. Short, D. Miller, and Y. Tang, J. Solid State Chem. **170**, 339 (2003).

[29] M. Soda, Y. Yasui, M. Ito, S. Iikubo, M. Sato, and K. Kakurai, J. Phys. Soc. Jpn. **73**, 2857 (2004).

[30] V. P. Plakhty, Yu. P. Chernenkov, S. N. Barilo, A. Podlesnyak, E. Pomjakushina, E. V. Moskvin, and S. V. Gavrilov, Phys. Rev. B **71**, 214407 (2005).

[31] D. D. Khalyavin, Phys. Rev. B **72**, 134408 (2005).

[32] C. Frontera, J. L. García-Muñoz, A. E. Carrillo, M. A. G. Aranda, I. Margiolaki, and A. Caneiro, Phys. Rev. B **74**, 054406 (2006).

[33] M. García-Fernández, V. Scagnoli, U. Staub, A. M. Mulders, M. Janousch, Y. Bodenthin, D. Meister, B. D. Patterson, A. Mirone, Y. Tanaka, T. Nakamura, S. Grenier, Y. Huang, and K. Conder, Phys. Rev. B **78**, 054424 (2008).

[34] D. Chernyshov, V. Dmitriev, E. Pomjakushina, K. Conder, M. Stingaciu, V. Pomjakushin, A. Podlesnyak, A. A. Taskin, and Y. Ando, Phys. Rev. B **78**, 024105 (2008).

[35] J.-E. Jørgensen and L. Keller, Phys. Rev. B **77**, 024427 (2008).

[36] D. P. Kozlenko, Z. Jirák, N. O. Golosova, and B. N. Savenko, Eur. Phys. J. B **70**, 327 (2009).

[37] N. Ishizawa, T. Asaka, T. Kudo, K. Fukuda, N. Abe, and T. Arima, J. Solid State Chem. **198**, 532 (2013).

[38] V. V. Volkov, D. C. Crew, Y. Zhu, and L. H. Lewis, Rev. Sci. Instrum. **73**, 2298 (2002).

[39] C. Frontera, J. L. García-Muñoz, A. Llobet, and M. A. G. Aranda, Phys. Rev. B **65**, 180405(R) (2002).

[40] See Supplemental Material at http://link.aps.org/supplemental/10.1103/PhysRevLett.110.125502 for the sample preparation for TEM and the measurements.

[41] J. Padilla-Pantoja, C. Frontera, O. Castaño, and J. L. García-Muñoz, Phys. Rev. B **81**, 132405 (2010).

[42] Yu. P. Chernenkov, V. P. Plakhty, V. I. Fedorov, S. N. Barilo, S. V. Shiryaev, and G. L. Bychkov, Phys. Rev. B **71**, 184105 (2005).

[43] A. A. Taskin and Y. Ando, Phys. Rev. Lett. **95**, 176603 (2005).

[44] J. Lejay, A. G. M. Jansen, P. Wyder, W. Bronger, and W. Kläui, Phys. Rev. B **43**, 8196 (1991).

[45] A. Bousseksou, K. Boukheddaden, M. Goiran, C. Consejo, M-L. Boillot, and J-P. Tuchagues, Phys. Rev. B **65**, 172412 (2002).

[46] S. Kimura, Y. Maeda, T. Kashiwagi, H. Yamaguchi, M. Hagiwara, S. Yoshida, I. Terasaki, and K. Kindo, Phys. Rev. B **78**, 180403(R) (2008).